

Coherent triplet excitation suppresses the heading error of the avian compass

This article has been downloaded from IOPscience. Please scroll down to see the full text article.

2010 New J. Phys. 12 085016

(<http://iopscience.iop.org/1367-2630/12/8/085016>)

View [the table of contents for this issue](#), or go to the [journal homepage](#) for more

Download details:

IP Address: 139.91.179.103

The article was downloaded on 21/09/2010 at 11:25

Please note that [terms and conditions apply](#).

Coherent triplet excitation suppresses the heading error of the avian compass

G E Katsoprinakis, A T Dellis and I K Kominis¹

Department of Physics, University of Crete, Heraklion 71103, Greece
and

Institute of Electronic Structure and Laser, Foundation for Research and
Technology, Heraklion 71110, Greece

E-mail: ikominis@iesl.forth.gr

New Journal of Physics **12** (2010) 085016 (13pp)

Received 14 May 2010

Published 27 August 2010

Online at <http://www.njp.org/>

doi:10.1088/1367-2630/12/8/085016

Abstract. Radical-ion pair reactions are currently understood to underlie the biochemical magnetic compass of migratory birds. It was recently shown that radical-ion pair reactions form a rich playground for the application of quantum-information-science concepts and effects. We will show here that the intricate interplay between the quantum Zeno effect and the coherent excitation of radical-ion pairs leads to an exquisite angular sensitivity of the reaction yields. This results in a significant and previously unanticipated suppression of the avian compass heading error, opening the way to quantum engineering precision biological sensors.

¹ Author to whom any correspondence should be addressed.

Contents

1. Introduction	2
2. The avian compass mechanism	3
2.1. Magnetic interactions	6
3. Definition of quantum states	6
4. Triplet excitation enhances the angular sensitivity of reaction yields	7
4.1. Explanation of the effect	7
5. Phenomenological versus quantum measurement theory	9
5.1. Phenomenological theory	9
5.2. Quantum measurement theory	9
6. Heading error	10
7. Is our model realistic?	10
8. Conclusions	11
References	11

1. Introduction

Quantum physics and biology have traditionally been considered to have in common nothing more than the obvious fact that the structure of matter, from atoms to bio-molecules, is determined by quantum mechanics. There is more to quantum physics, however, besides the ‘static’ energy eigenvalue spectrum of a collection of electrons and nuclei. The modern revolution in the physics of information, quantum information science, rests on two basic physical concepts: coherent superposition and entanglement. It is these two fundamentally non-classical concepts that drive the superb capabilities of quantum information processing.

The possibility that such quantum phenomena could be found to underlie the workings of biological systems [1] has been traditionally and intuitively considered to be remote if not absurd, because of another ever recurring concept of quantum physics: decoherence. The interaction of quantum systems with their environment makes coherent superpositions and entanglement very fragile, to the extent that any operational advantage stemming from them cannot be sustained for biological/biochemical time scales [2].

Recent years, however, have witnessed growing evidence pointing to the counter-intuitive notion that non-trivial quantum effects are indeed responsible for some exquisite capabilities of biological systems, often found to pose a severe challenge to man’s attempt to reproduce them. The main thrust of this progress is related to the role that quantum coherence plays in photosynthesis [3], in particular the intricate quantum machinery of the photosynthetic antennae, the role of which is to efficiently guide the excitonic energy [4]–[10] provided by the sun’s photons to the photosynthetic reaction center for further biochemical processing.

We will here focus on another biological system that was recently shown to exhibit non-trivial quantum effects: radical-ion pairs and their reactions. Radical-ion pair reactions are the basic ingredient of the field of spin chemistry [11]–[13], i.e. the effect of spin degrees of freedom on chemical reactions. Since the Zeeman interaction energy of an electron or a magnetic nucleus in a small magnetic field (e.g. the earth’s field of interest for this work) is several orders of magnitude smaller than the thermal energy at room temperature, spin degrees of freedom

were thought to be incapable of affecting chemical reactions. However, angular momentum conservation can amplify the effect of spin on the fate of a chemical reaction, as is the case in radical-ion pair reactions, leading to a multitude of physical and chemical effects that have been studied extensively over the last four decades, experimentally as well as theoretically.

Radical-ion pairs play a fundamental role in charge transfer-initiated reactions in photosynthetic reaction centers [14, 15]. Furthermore, radical-ion pair reactions are one of the two main mechanisms currently thought to explain avian magnetoreception [16]–[23], the biological compass that avian species use for navigation in the geomagnetic field, the other being the magnetic torque on biogenic magnetite particles [24, 25].

It was recently shown [26] that the fundamental description of radical-ion pair reactions following from quantum measurement theory reveals the actual presence of non-trivial quantum effects, such as the quantum Zeno effect [27]–[30]. In other words, this biochemical reaction of biological significance was shown to exhibit physical concepts and effects familiar from quantum information science and not accounted for by the previous, phenomenological theory of radical-ion pair reactions. Several other works followed, discussing the quantum physical aspects of radical-ion pair reactions [31, 32]. In particular, Jones and Hore [32] introduced a different approach to quantum measurement dynamics inherent in the recombination of radical-ion pairs, which, as the authors point out, largely reproduces the previous, phenomenological theory of radical-ion pair reactions. Thus the comparison of our predictions regarding the avian compass heading error that are presented in this work and are based on [26] against the predictions of the phenomenological theory is a simultaneous comparison against the predictions of [32].

In this work, we will study the angular precision or heading error of the avian compass, i.e. the precision in determination of the magnetic field inclination with respect to a local, molecule-fixed coordinate frame. We will focus on the strong measurement regime, i.e. the regime where the recombination rates of the radical-ion pair dominate the spin state evolution of the molecule. We will show that in this regime, the particular symmetry of a coherently excited triplet state and the breaking thereof by a magnetic field result in a surprisingly small heading error, completely unanticipated by the phenomenological theory of radical-ion pair reactions used until now. We will elucidate how quantum effects and concepts familiar from atomic physics can be used to gain a deeper understanding of this biochemical reaction, thus opening the possibility of quantum engineering biological sensors of exquisite capabilities.

2. The avian compass mechanism

Radical-ion pairs are formed by a charge transfer process following photo-excitation of a donor–acceptor dyad, leading to two molecular ions and two unpaired electrons. The latter can be either in the spin singlet or in the spin triplet state (figure 1). Magnetic interactions with the external magnetic field and hyperfine interactions with the molecule’s magnetic nuclei bring about a coherent singlet–triplet oscillation. At some random instant in time, the reaction is terminated, since the radical-ion pair undergoes charge recombination, leading to the reaction products. Angular momentum conservation enforces spin selectivity of the recombination process, i.e. singlet (triplet) radical-ion pairs recombine to singlet (triplet) neutral products. Radical-ion pair reactions are theoretically described by the $4n$ -dimensional spin density matrix ρ of the pertaining particles, where the factors 4 and $n = (2I_1 + 1)(2I_2 + 1) \dots (2I_k + 1)$ are the electron and nuclear spin multiplicities, respectively, and I_1, I_2, \dots, I_k are the nuclear spins

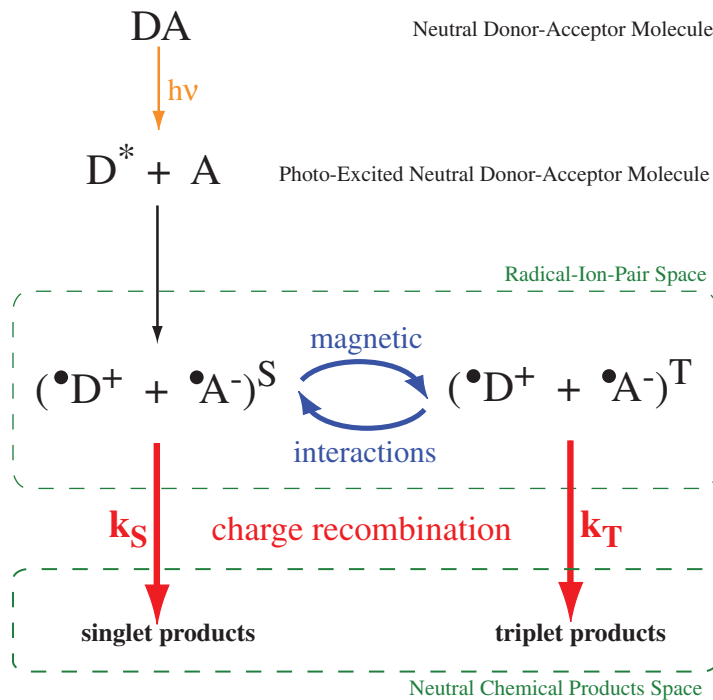


Figure 1. Schematic diagram of radical-ion pair reaction dynamics. A photon excites a donor–acceptor molecular dyad, which after a charge transfer process creates a radical-ion pair. The magnetic interactions of the two unpaired electrons (two dots) with the external magnetic field and the molecule’s magnetic nuclei bring about a coherent singlet–triplet conversion. This would go on forever if it were not for the charge-recombination process that transforms radical-ion pairs into neutral products. Angular momentum conservation enforces spin selectivity of the recombination, i.e. singlet (triplet) radical-ion pairs recombine to form singlet (triplet) chemical products. It is through this step that the small magnetic interaction energy scale can influence the fate of this chemical reaction amidst the much larger thermal energy.

of the k magnetic nuclei existing in the donor and acceptor molecules altogether. We will henceforth consider the simplest physically realizable radical-ion pair with just one nucleus (e.g. in the donor molecule) with spin-1/2, in which case the density matrix is eight dimensional (8D). This simple model obviously does not exhaust all the richness in the reaction dynamics provided by the presence of tens of magnetic nuclei, as is the case in naturally existing [21] or synthesized biomolecules [33], but it does include a lot of the basic physics involved and is numerically, and in some cases analytically, tractable.

It was recently shown [26] that the unconditional evolution of ρ following from quantum measurement theory is given by the Liouville equation,

$$d\rho/dt = -i[\mathcal{H}_m, \rho] - (k_S + k_T)(Q_S\rho + \rho Q_S - 2Q_S\rho Q_S), \quad (1)$$

where Q_S is the singlet state projection operator (the triplet state projection operator is Q_T and the completeness relation is $Q_S + Q_T = 1$, where 1 is, in the case we are considering, the 8D unit matrix). The first term in (1) is the unitary evolution due to the magnetic interactions, whereas

the second term describes the measurement-induced evolution due to the singlet (rate k_S) and triplet (rate k_T) charge recombination channel. The quantum measurement of the electron spin state is inherent in the radical-ion pair, induced by the singlet and triplet reservoirs. These are the vibrational excited states [26] of the neutral singlet and triplet product molecules. The rates k_S and k_T are determined by the molecular structure of the particular molecule under consideration [26].

The effect of charge recombination is the termination of the reaction. That is, at a random instant in time while oscillating between the singlet and triplet states, the radical-ion pair recombines through either the singlet or the triplet channel. This is described by the quantum jump equations [34],

$$\begin{aligned} dp_S &= 2k_S \langle Q_S \rangle dt, \\ dp_T &= 2k_T \langle Q_T \rangle dt, \end{aligned} \quad (2)$$

which give the probability of singlet and triplet recombinations taking place within the time interval between t and $t + dt$. For example, the probability of singlet recombination between t and $t + dt$ is equal to the probability $\langle Q_S \rangle = \text{Tr}\{\rho Q_S\}$ of the electron spin being in the singlet state times the probability of the jump $2k_S dt$.

Because radical-ion pairs recombine one way or another, their number $N(t)$ evolves according to

$$\frac{dN(t)}{dt} = -(2k_S \langle Q_S \rangle + 2k_T \langle Q_T \rangle) N(t). \quad (3)$$

The solution of the above equation is, since $\langle Q_S \rangle + \langle Q_T \rangle = 1$,

$$N(t) = N_0 e^{-2k_S t} e^{-2(k_T - k_S) \int_0^t \langle Q_T \rangle d\tau}, \quad (4)$$

with $N_0 = N(t = 0)$ being the initial number of radical-ion pairs. The singlet and triplet reaction yields are given by

$$Y_S[\%] = \frac{100}{N_0} \int_0^\infty dp_S(t) N(t), \quad (5)$$

$$Y_T[\%] = \frac{100}{N_0} \int_0^\infty dp_T(t) N(t), \quad (6)$$

and obviously satisfy $Y_S + Y_T = 100\%$. The time evolution of the expectation values $\langle Q_S \rangle = \text{Tr}\{\rho(t) Q_S\}$ and $\langle Q_T \rangle = \text{Tr}\{\rho(t) Q_T\}$ depends on the solution $\rho(t)$ of the Liouville equation (1). Hence, information about the external magnetic field is imprinted on the reaction yields through the influence of the magnetic Hamiltonian \mathcal{H}_m on $\rho(t)$. For completeness, we recapitulate the phenomenological density matrix equation previously used to describe the dynamics of radical-ion pair reactions,

$$\frac{d\rho}{dt} = -i[\mathcal{H}_m, \rho] - k_S(\rho Q_S + Q_S \rho) - k_T(\rho Q_T + Q_T \rho). \quad (7)$$

In the following, we will compare the predictions of the recently developed quantum measurement theory of radical-ion pair reactions against those of the phenomenological theory, as the latter will be shown to greatly underestimate the capabilities of the avian compass in certain regimes of the relevant parameter and state space.

2.1. Magnetic interactions

The magnetic interactions within the radical-ion pair that we will consider are the Zeeman interaction of the two unpaired electrons (nuclear Zeeman interaction is negligible) with the external magnetic field,

$$\mathcal{H}_Z = \omega(\sin \theta \cos \phi S_x + \sin \theta \sin \phi S_y + \cos \theta S_z), \quad (8)$$

where $\omega = \gamma B$, with $\gamma = 2.8 \text{ MHz G}^{-1}$, $\mathbf{S} = \mathbf{s}_1 + \mathbf{s}_2$ is the total electron spin and θ, ϕ describe the direction of the field in the local coordinate frame and the hyperfine coupling with the single nucleus,

$$\mathcal{H}_{\text{hf}} = \mathbf{I} \cdot \mathbf{A} \cdot \mathbf{s}_1, \quad (9)$$

where \mathbf{A} is the hyperfine coupling tensor. For the following calculations, we will consider a diagonal hyperfine tensor with $A_{xx} = a_x$, $A_{yy} = a_y$ and $A_{zz} = a_z$. Thus, the magnetic Hamiltonian that will be used is

$$\mathcal{H}_m = \mathcal{H}_Z + a_x I_x s_{1x} + a_y I_y s_{1y} + a_z I_z s_{1z}. \quad (10)$$

Finally, the projection operators to the singlet and triplet subspaces are

$$Q_S = 1/4 - \mathbf{s}_1 \cdot \mathbf{s}_2, \quad (11)$$

$$Q_T = 3/4 + \mathbf{s}_1 \cdot \mathbf{s}_2. \quad (12)$$

3. Definition of quantum states

The electronic spin space of the pair of electrons is spanned by the singlet and the three triplet basis states, which in the usual representation of the $\hat{\mathbf{z}}$ -axis being the quantization axis are

$$|S\rangle = \frac{1}{\sqrt{2}}(|\uparrow, \downarrow\rangle - |\downarrow, \uparrow\rangle), \quad (13)$$

$$|T_+\rangle_z = |\uparrow, \uparrow\rangle,$$

$$|T_0\rangle_z = \frac{1}{\sqrt{2}}(|\uparrow, \downarrow\rangle + |\downarrow, \uparrow\rangle), \quad (14)$$

$$|T_-\rangle_z = |\downarrow, \downarrow\rangle.$$

Being a zero spin state, the singlet state is invariant under rotations, but the triplet states are not. In the following, triplet states along different quantization axes will be used. They are obtained through rotations of the $\hat{\mathbf{z}}$ -states by $\pi/2$ about the $\hat{\mathbf{y}}$ -axis ($\hat{\mathbf{x}}$ -states) and a consecutive rotation by $\pi/2$ about the $\hat{\mathbf{z}}$ -axis ($\hat{\mathbf{y}}$ -states),

$$|T_0\rangle_x = \frac{1}{\sqrt{2}}(-|T_+\rangle_z + |T_-\rangle_z), \quad (15)$$

$$|T_{\pm}\rangle_x = \frac{1}{2}(|T_+\rangle_z \pm \sqrt{2}|T_0\rangle_z + |T_-\rangle_z),$$

$$|T_0\rangle_y = -\frac{1}{\sqrt{2}}(|T_+\rangle_z + |T_-\rangle_z), \quad (16)$$

$$|T_{\pm}\rangle_y = \frac{1}{2}(|T_+\rangle_z \pm i\sqrt{2}|T_0\rangle_z - |T_-\rangle_z).$$

In the following, we will consider that the reaction starts out from the triplet manifold. As is usual in such calculations, we take the nuclear spin to be initially uncorrelated with the electron spins. Hence, the initial spin density matrix can be written as

$$\rho(t=0) = \rho_n \otimes \rho_e, \quad (17)$$

where $\rho_n = 1/2$ is the fully mixed nuclear spin state and ρ_e is the spin state of the two electrons. If the latter are created in a spin-correlated state of the form

$$|\psi\rangle = \alpha|T_+\rangle + \beta|T_0\rangle + \gamma|T_-\rangle, \quad (18)$$

then the initial density matrix of the radical-ion pair is

$$\rho = \rho_n \otimes |\psi\rangle\langle\psi|. \quad (19)$$

4. Triplet excitation enhances the angular sensitivity of reaction yields

We will now state the main result of this work and then explain it in detail. We calculate the triplet reaction yield as a function of the angle θ that the magnetic field makes with the \hat{z} -axis, while rotating on the x - z -plane (that is, in (10), we set $\phi = 0$ and let θ vary between 0 and 2π). We do the calculation for two cases: (i) the initial state is the singlet state $\rho(t=0) = Q_S/2$ and (ii) the initial state is a coherent triplet state. For each of these two cases, we consider (a) the traditional regime of equal recombination rates $k_S = k_T$ and (b) the regime of asymmetric recombination rates, in which case the quantum measurement effects of the molecule's spin state evolution are dominant. In particular, in case (i), where the radical-ion pair starts out from the singlet state, we have $k_T \gg k_S$, whereas in case (ii), where the molecule starts out from the triplet manifold, we take $k_S \gg k_T$. In figures 2(a) and (b), we plot the angular sensitivity of the triplet yield when the initial state is a singlet state for the two cases of equal and asymmetric recombination rates, respectively. Similarly, figures 2(c) and (d) depict the same calculation but starting out from the triplet manifold. It is clearly seen that the results following from the phenomenological theory are qualitatively similar to the predictions of quantum measurement theory in all but the case of figure 2(d), where the initial state is the triplet cat state $|T_0\rangle_y = (|++\rangle + |--\rangle)/\sqrt{2}$, and the recombination rates fall well into the quantum Zeno regime $k_S \gg k_T$. This case predicts an exquisite angular sensitivity $\Delta Y \equiv |Y_T(\pi/2) - Y_T(0)|$ of roughly 50%, ten times higher than what would be anticipated from the phenomenological theory.

4.1. Explanation of the effect

Towards explaining the effect just described, we first plot (figure 3(a)) the triplet yield as a function of the singlet recombination rate for various initial states of the radical-ion pair and for zero magnetic field, again for a hyperfine coupling with \hat{z} -anisotropy, i.e. in (10) we take $a_z \neq 0$ and $a_x = a_y = 0$. It is seen that certain initial states do not undergo singlet-triplet mixing and result in 100% triplet yield. Indeed, the states $|T_{\pm}\rangle_q$ do not evolve under the action of \mathcal{H}_m having $\hat{\mathbf{q}}$ -anisotropy, where $q = x, y, z$ (here $q = z$). This is so because $[\mathcal{H}_m, \rho_{\pm}^{(q)}] = 0$, with $\rho_{\pm}^{(q)}$ being the density matrix corresponding to $|T_{\pm}\rangle_q$ according to (19). The same holds true when a magnetic field parallel to $\hat{\mathbf{q}}$ is applied, since then the states $|T_{\pm}\rangle_q$ are eigenstates of S_q , the $\hat{\mathbf{q}}$ -component of the total electron spin.

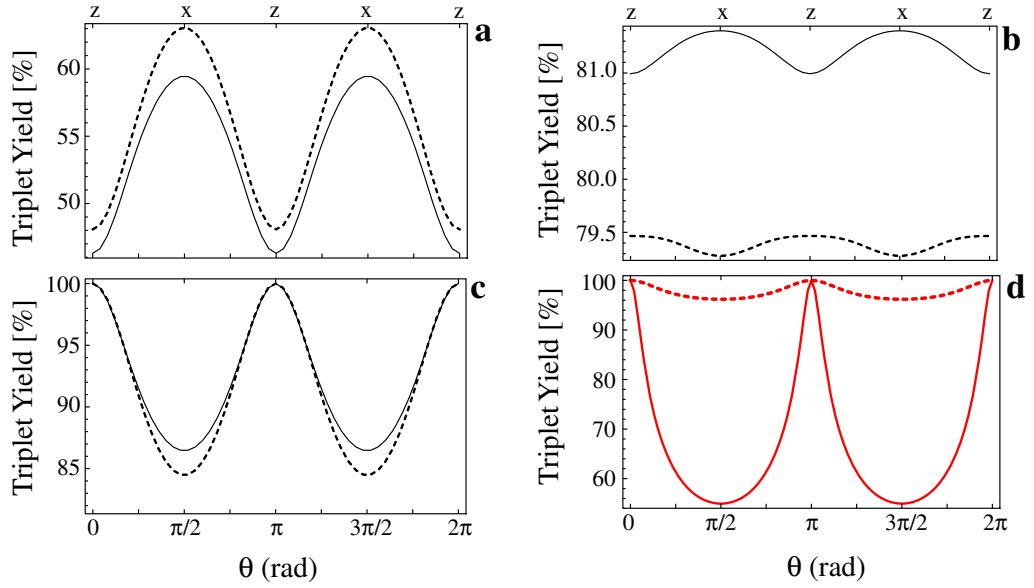


Figure 2. Angular sensitivity of triplet yield for a \hat{z} -anisotropic hyperfine coupling. In (a) and (b) the radical-ion pair starts out in the singlet state, whereas in (c) and (d) the initial state is the triplet cat state, $|T_0\rangle_y$. The left column (a and c) is the traditional $k_S = k_T$ regime with $k_S = k_T = 0.5$ MHz, whereas the right column is the quantum Zeno regime with asymmetric recombination rates. In (b) $k_S = 0.3$ MHz, $k_T = 3$ MHz, and in (d) $k_S = 35$ MHz, $k_T = 0.5$ MHz. Solid (dashed) lines are the results following from the quantum-measurement (phenomenological) theory. For all plots, the hyperfine coupling was $a_z = 10$ MHz and the magnetic field $B = 0.5$ G.

From (15) it is seen that the $|T_0\rangle_{p \neq q}$ states are linear combinations of $|T_{\pm}\rangle_q$ and should also be unaffected, as is indeed evident in figure 3. In fact, any linear combination of $|T_{\pm}\rangle_q$ will yield 100% triplet products. On the other hand, the zero-projection triplet state, $|T_0\rangle_q$, does not commute with \mathcal{H}_m having $\hat{\mathbf{q}}$ -anisotropy and leads to a non-zero singlet yield.

The symmetry of the system is broken when a magnetic field with at least one non-zero component perpendicular to $\hat{\mathbf{q}}$ is applied. In this case, the $|T_{\pm}\rangle_q$ states rotate about the perpendicular component of the field, mixing into the state of the system a $|T_0\rangle_q$ component, which, as noted above, leads to singlet products. This can be seen in figure 3(b), where the triplet yield is plotted against the singlet recombination rate for a $|T_0\rangle_y$ initial state, and a small magnetic field along either $\hat{\mathbf{z}}$ or $\hat{\mathbf{x}}$. As expected, when $\mathbf{B} \parallel \hat{\mathbf{z}}$ the input state $|T_0\rangle_y$ (composed of $|T_{\pm}\rangle_z$) leads to 100% triplet products. In contrast, when the magnetic field is aligned perpendicular to $\hat{\mathbf{z}}$ (here along $\hat{\mathbf{x}}$), a non-zero singlet yield appears.

Figure 3(b) embodies the main result of this work, i.e. the enhanced angular sensitivity of the system: a 90° rotation of a small magnetic field produces a large triplet yield change, which in fact increases with k_S , the singlet recombination rate. The exact opposite is the prediction of the phenomenological theory. We will now address the root of this fundamental difference between the predictions of the two theories.

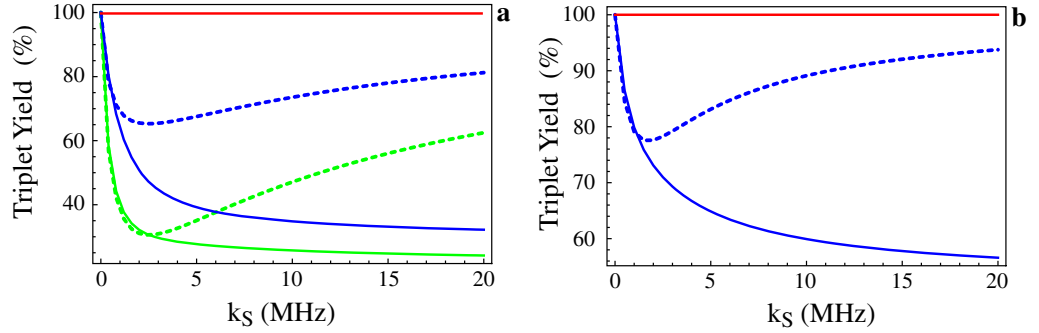


Figure 3. Triplet yield as a function of the singlet recombination rate for a \hat{z} -anisotropic hyperfine coupling and for various initial states. For all plots, $a_z = 10$ MHz and $k_T = 0.5$ MHz. Solid (dashed) lines for the quantum-measurement (phenomenological) theory. (a) Red line for $|T_{\pm}\rangle_z$ and $|T_0\rangle_{x(y)}$, green for $|T_0\rangle_z$, blue for $|T_{\pm}\rangle_{x(y)}$ and $B = 0$. (b) For an initial state $|T_0\rangle_y$ and $B = 0.5$ G parallel to the \hat{z} (red) or \hat{x} (blue) axis.

5. Phenomenological versus quantum measurement theory

For a zero magnetic field, we can find an analytic solution for the expectation value $\langle Q_S \rangle$ for both theories. The qualitative conclusions following thereof are valid also for small magnetic fields.

5.1. Phenomenological theory

Starting out with an initial state $|T_0\rangle_z$, it follows from (7) that

$$\langle Q_S(t) \rangle = \frac{1}{2} \frac{(a_z/2)^2}{\kappa^2} [\cosh(\kappa t) - 1] e^{-(k_S + k_T)t}, \quad (20)$$

where $\kappa \equiv \sqrt{(k_S - k_T)^2 - (a_z/2)^2}$. For very large k_S , we can approximate the previous exact time evolution by

$$\langle Q_S(t) \rangle \approx \frac{1}{4} \frac{(a_z/2)^2}{k_S^2} [e^{-k_T t} - e^{-k_S t}], \quad (21)$$

leading to a singlet yield

$$Y_S = 2k_S \int_0^\infty dt \langle Q_S(t) \rangle \approx \frac{1}{2} \frac{(a_z/2)^2}{k_T k_S}. \quad (22)$$

Clearly, $Y_S \rightarrow 0$ as $k_S \rightarrow \infty$. Physically, this corresponds to a situation where, starting from a triplet state, the high singlet recombination rate instantly destroys the coherence created between $|T_0\rangle_z$ and $|S\rangle$ by the hyperfine interaction, before it has the time to be transformed into a real singlet population. This state of affairs has been analyzed in [35].

5.2. Quantum measurement theory

In contrast, the solution for $\langle Q_S(t) \rangle$ following from quantum measurement theory (equations (1) and (2)) is

$$\langle Q_S(t) \rangle = \frac{1}{2} - \frac{1}{2} \left[\cosh(\kappa' t) + \frac{k}{2\kappa'} \sinh(\kappa' t) \right] e^{-kt/2}, \quad (23)$$

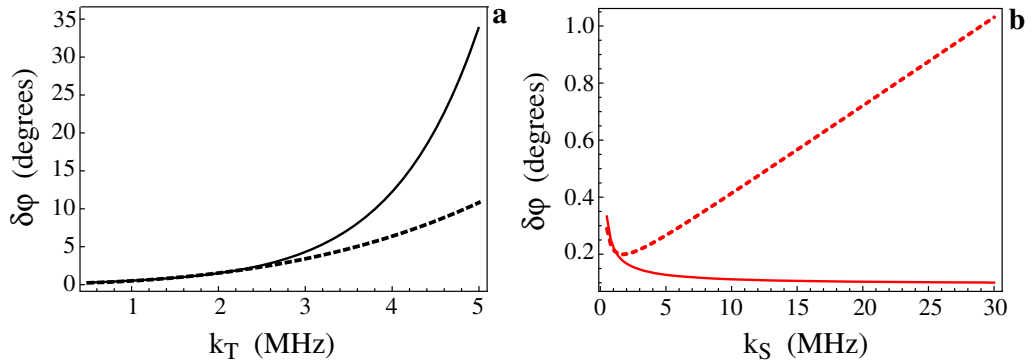


Figure 4. Avian compass heading error for a \hat{z} -anisotropic hyperfine coupling. For both plots, $a_z = 10$ MHz and $B = 0.5$ G. (a) Heading error as a function of k_T with a singlet initial state and $k_S = 0.5$ MHz. (b) Heading error as a function of k_S for a $|T_0\rangle_y$ initial state and $k_T = 0.5$ MHz. Solid (dashed) lines for the quantum-measurement (phenomenological) theory.

where $k = k_S + k_T$ is the total measurement rate and $\kappa' \equiv \sqrt{k^2 - a_z^2}/2$. For large k_S , this simplifies to

$$\langle Q_S(t) \rangle \approx \frac{1}{2}(1 - e^{-k_T t/2}). \quad (24)$$

Essentially, deep in the quantum Zeno regime, no matter how large k_S is, the population is always transferred to the singlet state and singlet products appear. This is due to the spin state delocalization produced by the strong measurement dynamics inherent in the radical-ion pair recombination process [36].

6. Heading error

Finally, in figure 4, we depict the heading error $\delta\varphi \equiv (\pi/2)\delta Y/[Y_T(0) - Y_T(\pi/2)]$, using a particular and realistic [37] value of the reaction yield measurement precision $\delta Y = 0.05\%$. A singlet initial state is invariant under rotations and hence there is no particular anisotropy direction along which the singlet yield is 100%, as is the case with the triplet initial state, explained in section 4. Thus, the pronounced yield dependence on the symmetry-breaking magnetic field is missing, and the heading error is large and increases the deeper into the quantum Zeno regime (i.e. $k_T \gg k_S$) we go. This state of affairs is shown in figure 4(a). In contrast, starting out from the triplet state, the heading error is suppressed for increasing k_S and it is an order of magnitude smaller than what would be anticipated from the phenomenological theory. This is depicted in figure 4(b), where it is seen that the heading error can reach rather spectacular values, less than 0.1° .

7. Is our model realistic?

The model we have analyzed in this work is a proof of principle. It opens the way to applications of quantum control methods in biochemical reactions. For the moment, our model might be unrealistic, but the aim of this work is to demonstrate what is the possible behavior of this biochemical system allowed by the underlying theory.

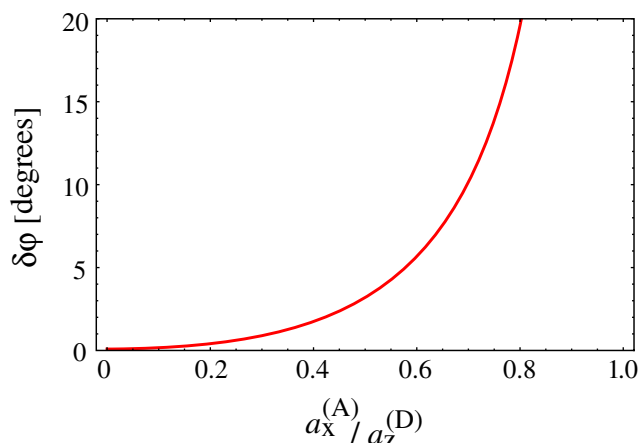


Figure 5. Avian compass heading error as a function of a_X^A/a_z^D for a $|T_0\rangle_y$ initial state with $k_S = 35$ MHz, $k_T = 0.5$ MHz and $a_z^D = 10$ MHz.

Clearly, there are several questions that this work might raise. How are our results altered if we add one or more nuclei, possibly with different anisotropy axes? In figure 5, we plot the change in the heading error that takes place if we add another spin-1/2 nucleus in the acceptor molecule, having an anisotropy along the \hat{x} -axis. As expected, for low values of a_X^A , our results are valid, but for higher a_X^A , the angular precision of the system is suppressed. However, there is no law of physics prohibiting the existence of radical-ion pairs having the coupling that will realize the conclusions of this work. Another question is how to realize the particular initial state. As mentioned in [38], although singlet precursors are what we usually consider in spin chemistry, in many cases the reaction starts out in the triplet state. How to engineer a particular coherent superposition in the triplet state manifold is then a matter of applying, by now, very mature methods of NMR. So, again, our results are physically allowed and experimentally accessible.

8. Conclusions

We have analyzed the heading error of the avian compass for different initial state configurations. We have elucidated and explained cases where the predictions of the phenomenological theory of radical-ion pair reactions used until now severely underestimated the actual capabilities offered by the quantum dynamics of the radical-ion pair magnetoreception model. This work opens the way to investigate the application of well-established methods and techniques of quantum control in a biologically significant system.

References

- [1] Davies P C W 2004 Does quantum mechanics play a non-trivial role in life? *Biosystems* **78** 69
- [2] Abbott D *et al* 2008 Plenary debate: quantum effects in biology: trivial or not? *Fluctuat. Noise Lett.* **8** C5
- [3] Ritz T, Damjanovic A and Schulten K 2002 The quantum physics of photosynthesis *ChemPhysChem* **3** 243
- [4] Engel G S *et al* 2007 Evidence for wavelike energy transfer through quantum coherence in photosynthetic systems *Nature* **446** 782

- [5] Lee H, Cheng Y C and Fleming G R 2007 Coherence dynamics in photosynthesis: protein protection of excitonic coherence *Science* **316** 1462
- [6] Mohseni M, Rebentrost P, Lloyd S and Aspuru-Guzik A 2008 Environment-assisted quantum walks in photosynthetic energy transfer *J. Chem. Phys.* **129** 174106
- [7] Plenio M B and Huelga S F 2008 Dephasing-assisted transport: quantum networks and biomolecules *New J. Phys.* **10** 113019
- [8] Olaya-Castro A, Lee C F, Olsen F F and Johnson N F 2008 Efficiency of energy transfer in a light-harvesting system under quantum coherence *Phys. Rev. B* **78** 085115
- [9] Wilde M M, McCracken J M and Mizel A 2010 Could light harvesting complexes exhibit non-classical effects at room temperature? *Proc. R. Soc. A: Math. Phys.* **466** 1347
- [10] Collini E, Wong C Y, Wilk K, Curmi P M G, Brumer P and Scholes G D 2010 Coherently wired light-harvesting in photosynthetic marine algae at ambient temperature *Nature* **463** 644
- [11] Steiner U and Ulrich T 1989 Magnetic field effects in chemical kinetics and related phenomena *Chem. Rev.* **89** 51
- [12] Brocklehurst B 2002 Magnetic fields and radical reactions: recent developments and their role in nature *Chem. Soc. Rev.* **31** 301
- [13] Timmel C R and Henbest K B 2004 A study of spin chemistry in weak magnetic fields *Phil. Trans. R. Soc. A* **362** 2573
- [14] Boxer S G 1983 Model reactions in photosynthesis *Biochim. Biophys. Acta* **726** 265
- [15] Boxer S G, Chidsey C E D and Roelofs M G 1983 Magnetic-field effects on reaction yields in the solid-state—an example from photosynthetic reaction centers *Ann. Rev. Phys. Chem.* **34** 389
- [16] Schulten K 1982 Magnetic field effects in chemistry and biology *Adv. Solid State Phys.* **22** 61
- [17] Wiltschko W and Wiltschko R 1996 Magnetic orientation in birds *J. Exp. Biol.* **199** 29
- [18] Timmel C R, Till U, Brocklehurst B, McLaughlan K A and Hore P J 1998 Effects of weak magnetic fields on free radical recombination reactions *Mol. Phys.* **95** 71
- [19] Ritz T, Adem S and Schulten K 2000 A model for photoreceptor-based magnetoreception in birds *Biophys. J.* **78** 707
- [20] Wiltschko W and Wiltschko R 2005 Magnetic orientation and magnetoreception in birds and other animals *J. Comput. Physiol. A* **191** 675
- [21] Solov'yov I A, Chandler D E and Schulten K 2007 Magnetic field effects in *Arabidopsis thaliana* cryptochrome-1 *Biophys. J.* **92** 2711
- [22] Maeda K *et al* 2008 Chemical compass model of avian magnetoreception *Nature* **453** 387
- [23] Rodgers C T and Hore P J 2009 Chemical magnetoreception in birds: the radical pair mechanism *Proc. Natl Acad. Sci. USA* **106** 353
- [24] Lohmann K J and Johnsen S 2000 The neurobiology of magnetoreception in vertebrate animals *Trends Neurosci.* **23** 153
- [25] Johnsen S and Lohmann K J 2005 The physics and neurobiology of magnetoreception *Nat. Rev. Neurosci.* **6** 703
- [26] Kominis I K 2009 Quantum Zeno effect explains magnetic-sensitive radical-ion-pair reactions *Phys. Rev. E* **80** 056115
- [27] Misra B and Sudarshan E C G 1977 The Zeno's paradox in quantum theory *J. Math. Phys.* **18** 756
- [28] Itano W M, Heinzen D J, Bollinger J J and Wineland D J 1990 Quantum Zeno effect *Phys. Rev. A* **41** 2295
- [29] Facchi P and Pascazio S 2008 Quantum Zeno dynamics: mathematical and physical aspects *J. Phys. A: Math. Theor.* **41** 493001
- [30] Erez N, Gordon G, Nest M and Kurizki G 2008 Thermodynamic control by frequent quantum measurements *Nature* **452** 724
- [31] Cai J M, Guerreschi G G and Briegel H J 2010 Quantum control and entanglement in the avian compass *Phys. Rev. Lett.* **104** 220502

- [32] Jones J A and Hore P J 2010 Spin-selective reactions of radical pairs act as quantum measurements *Chem. Phys. Lett.* **488** 90
- [33] Kuciauskas D, Lidell P A, Moore A L, Moore T A and Gust D 1998 Magnetic switching of charge separation lifetimes in artificial photosynthetic reaction centers *J. Am. Chem. Soc.* **120** 10880
- [34] Wiseman H M 1996 Quantum trajectories and quantum measurement theory *Quantum Semiclass. Opt.* **8** 205
- [35] Berdinskii V L and Yakunin I N 2008 Chemical Zeno effect and its manifestations *Dokl. Phys. Chem.* **421** 163
- [36] Gurvitz S A 1997 Measurements with a noninvasive detector and dephasing mechanism *Phys. Rev. B* **56** 15215
- [37] Weaver J C, Vaughan T E and Astumian R D 2000 Biological sensing of small field differences by magnetically sensitive chemical reactions *Nature* **405** 707
- [38] Woodward J R, Timmel C R, McLauchlan K A and Hore P J 2001 Radio frequency magnetic field effects on electron-hole recombination *Phys. Rev. Lett.* **87** 077602